THE ASTRONOMICAL JOURNAL, 117:1845–1851, 1999 April

ROSAT HIGH RESOLUTION IMAGER IDENTIFICATIONS OF SUSPECTED STELLAR SOURCES FROM THE *EINSTEIN* SLEW SURVEY

J. R. CHISHOLM[1]
Department of Physics and Astronomy, Northwestern University, 2131 Sheridan Road, Evanston, IL 60208-2900
F. R. HARNDEN, JR., AND J. F. SCHACHTER
Harvard-Smithsonian Center for Astrophysics, 60 Garden Street, Cambridge, MA 02138
G. MICELA AND S. SCIORTINO
Osservatorio Astronomico di Palermo, Piazza del Parlamento 1, I-90134 Palermo, Italy
AND
F. FAVATA
Astrophysics Division, European Space Agency, Postbus 299, NL-2200 AG Noordwijk, Netherlands
Received 1998 October 12; accepted 1998 December 22

ABSTRACT

We present analysis of a series of *ROSAT* High Resolution Imager (HRI) observations of 16 X-ray detections from the *Einstein* Slew Survey (ESS). The data were taken to resolve ambiguous ESS identifications based on optical spectroscopy. For 10 of the 16 detections, the previous identification has been confirmed—six with solar-type stars (spectral types F–K), one each with a cataclysmic variable, a B2 V, a dMe star, and one with a BL Lac object. For another detection, two potential counterparts are unresolvable even with the HRI. The HRI does resolve two other ESS detections into two distinct X-ray sources, but no HRI source is found for the remaining three X-ray detections. HRI-derived fluxes are consistent with those measured by the *ROSAT* All-Sky Survey for their 12 common detections, and improved positions are obtained for these sources. We calculate values of f_X/f_V and L_X for these stars where possible and find values consistent with those expected for corresponding spectral types.

Key word: X-rays

1. INTRODUCTION

The launch of the *Einstein Observatory* (Giacconi et al. 1979) in 1978 ushered in a new era in X-ray astronomy. Grazing-incidence imaging made this the first telescope with adequate sensitivity and spatial resolution to detect X-ray emission from normal stars. *Einstein* discovered nearly 5000 X-ray sources (Harris et al. 1993) in approximately 4000 pointed observations with the Imaging Proportional Counter (IPC; Gorenstein, Harnden, & Fabricant 1981). Roughly a quarter of these sources were stellar in origin. Data were also collected when the satellite was moving (or "slewing") from one pointed target to another. Although insufficient computing resources initially kept these data from being reduced, this task was later taken up by Elvis et al. (1992) to produce the *Einstein* Slew Survey (ESS). The ESS contains 809 X-ray sources, 313 of them previously unknown as X-ray emitters.

The initial identifications of ESS sources, performed on the basis of approximate position coincidence with objects present in catalogs at optical and other wavelengths, revealed that about 230 ESS sources had likely stellar counterparts (Elvis et al. 1992; Plummer et al. 1992). Because of the rapid slewing motion and poor statistics, the ESS had limited ability to localize sources (a 95% error radius of $\sim 2'$), as compared with the IPC pointed observations (and later missions). This made it difficult in many cases to obtain clear-cut identifications of the counterparts for the X-ray sources, notably when several potential stellar counterparts fell in the X-ray error circle. To resolve these ambiguities and provide a set of unique identifications, an extensive program of spectroscopic optical observations of potential stellar counterparts to ESS X-ray sources was carried out. These observations, which searched for signs of activity in the optical spectra of the potential counterparts (i.e., Ca II and Balmer emission) and measured rotational velocities, yielded unique identifications in most cases (Schachter et al. 1996, hereafter SRSFSB), which made it possible to do a study of the characteristics of the detected stellar population (Favata et al. 1995).

For a few cases, however, optical spectroscopy did not yield a unique counterpart, either because more than one star in the X-ray error circle showed signs of activity or because no optically active counterpart was found down to magnitudes compatible with the f_X/f_V ratio of coronal X-ray sources. Cases for which an A-type star appeared to be the only possible counterpart were of particular interest, because such stars are not known to be coronal sources. While dubious, such identifications would be quite interesting if confirmed.

For a small group of ESS X-ray detections, a program of short *ROSAT* High Resolution Imager (HRI; Zombeck et al. 1990) observations was begun with the aim of uniquely identifying optical counterparts at the X-ray positions by exploiting the HRI spatial resolution of a few arcseconds (David et al. 1997).[2] Here we present the results of the HRI-based counterpart identification program for 16 ESS sources. Our paper is structured as follows: Section 2 outlines the HRI observations and § 3 describes the analysis techniques used to identify the sources. In § 4 we give pertinent identification information for the individual sources.

[1] Summer Intern, Smithsonian Astrophysical Observatory.

[2] Available on-line at http://hea-www.harvard.edu/rosat/rsdc_www/hricalrep.html.

TABLE 1

JOURNAL OF OBSERVATIONS

ROR[a]	Date(s)	Exposure (s)	Target
201418H	1994 Mar 27	3136	1ES 0640+059
201419H	1994 Sep 5, 12	2101	1ES 0426−131
201435H	1994 Mar 26	1511	1ES 0629+068
201846H	1995 Feb 26, 28	7990	1ES 0437−046
201848H	1995 Apr 1	2200	1ES 0524−711
201849H	1995 Apr 2	1812	1ES 0629+068
201850H	1995 Mar 30, 31	4877	1ES 0640+059
201851H	1995 Apr 3	2036	1ES 0637−614
201852H	1995 Feb 3	898	1ES 1126−610
201852H-1	1996 Jan 14	1060	1ES 1126−610
201853H	1995 Feb 22	1148	1ES 1339−688
201854H	1995 Feb 26	1113	1ES 1456−400
201855H	1995 Jul 28, 29	3870	1ES 0237−531
201856H	1995 Jul 10, 13	4751	1ES 1002−559
201858H	1995 Aug 20	235	1ES 1147−625
201859H	1995 Aug 18	1541	1ES 0717−572
201860H	1995 Jul 7	3018	1ES 1212+078
201861H	1995 Aug 12, 13	2073	1ES 1414−197
201862H	1995 Aug 18	1281	1ES 1437−252

[a] *ROSAT* Observation Request.

Following the discussion in § 5 our results are summarized in § 6.

2. OBSERVATIONS

The data set consists of the 19 separate *ROSAT* HRI observations listed in Table 1 that were carried out from 1994 to 1996. With the exception of three observations of the S Mon region being studied by Flaccomio et al. (1999), these comprise all HRI pointings performed in the context of our identification program of ESS stellar counterparts. Each of the 16 ESS sources considered here was observed in either AO-4 or AO-5, with three of them observed in both periods. Because these HRI observations were planned to ensure detection for the X-ray intensities inferred from the ESS, they were mostly of short duration. Since most of the targets were scheduled as priority C, however, some were observed for only a fraction of the originally requested time.

3. DATA ANALYSIS

The HRI data were reduced using the standard *ROSAT* analysis system, which performs source detection and location and also suggests tentative identifications of sources with counterparts from known catalog objects (outlined in the *ROSAT* Data Products Guide, Downes et al. 1994). Typical HRI locations have uncertainties the order of $\sim 6''$, although in some cases the errors can be as large as $10''$ (David et al. 1997). A wavelet analysis source detection algorithm (Damiani et al. 1997) was also applied to the data and yielded the same results as the standard analysis.

The HRI observations resulted in high-confidence HRI source detections within $2'$ of the targeted position for 14 of the 16 ESS sources discussed here. One ESS source (1ES 1126−610) produced a low-confidence HRI source detection outside of $2'$ of the targeted position in both of its two observations (each about 1 ks in duration). For another ESS source (1ES 1437−252), no HRI X-ray source was detected.

For each field, the *ROSAT* All-Sky Survey (RASS) Bright Source Catalogue (BSC; see Voges et al. 1996) was searched

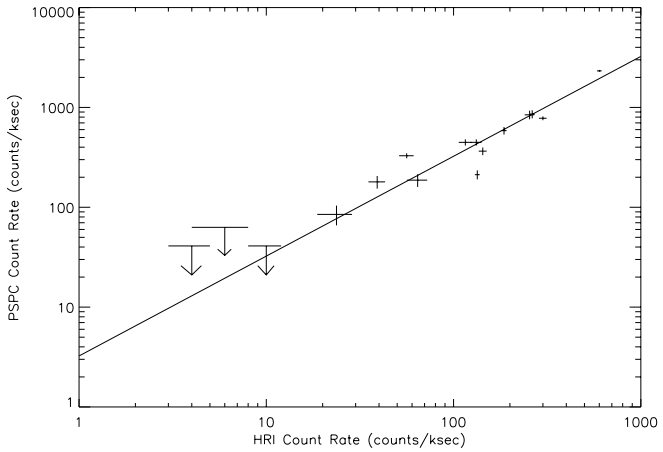

FIG. 1.—PSPC vs. HRI count rates for 13 HRI sources (one of which was observed twice) having RASS counterparts. The line is a least χ^2 linear fit, forced to include the origin PSPC = (3.24 ± 0.05) HRI, with both rates in counts ks^{-1}; 1 σ error bars are plotted for detected sources, and upper limits are shown at the RASS threshold rate for HRI sources with no detected RASS source.

within a $2'$ radius of the position of each HRI detection. All RASS sources found within this area were unique and were located less than $25''$ from the HRI position. Given that typical RASS position errors ($\sim 30''$) are larger than those of the HRI, this matching radius provides high confidence that the counterparts were correctly identified. Those HRI sources that did not have a RASS BSC counterpart within this $2'$ circle also did not have a RASS BSC source within $15'$, thus excluding ambiguities. While in most cases the shorter RASS exposures performed with the Position Sensitive Proportional Counter (PSPC; Pfeffermann et al. 1986) do not provide as much sensitivity as the pointed HRI observations, the RASS BSC does provide a consistency check for the count rates from the HRI and a check for source variability. The count rates for the HRI and PSPC are strongly correlated, providing a useful way of predicting PSPC count rates from HRI count rates. Figure 1 shows the relation between the count rates of the HRI and PSPC for those sources detected by both instruments. For HRI sources that did not have a RASS counterpart, PSPC count rates and photon counts are predicted to determine whether the source was below the PSPC detection threshold and thus whether its absence from the RASS is consistent with the count rate from the HRI source. The BSC has a detection threshold of 15 photons (see Voges et al. 1996); RASS exposure times for the sky were obtained from W. Voges (1997, private communication) and the BSC.[3]

To identify the actual counterpart to the HRI sources, we compared the optical information obtained in the framework of the SRSFSB program with the information available in the literature about sources in the ESS error circle (obtained by searching the SIMBAD database) and with the known properties of these X-ray sources as seen previously (from the HEASARC database). The *Hubble Space Telescope* Guide Star Photometric Catalog (Lasker et al. 1988) was also used for the field of 1ES 1414−197.

[3] RASS exposure times are calculated for positions without a RASS BSC source by looking in a 2° circle around the position for detected RASS BSC sources and interpolating an exposure time from nearby detected sources. These are in good agreement with the more accurate times obtained directly from W. Voges (1997, private communication).

To calculate a conversion factor from HRI count rate to flux, we assume a Raymond-Smith spectrum with no interstellar absorption and kT between 0.1 and 1 keV, which is appropriate for stellar sources; this conversion factor is 2×10^{-11} ergs cm^{-2} count^{-1}. X-ray–to–visual flux ratios and X-ray luminosities are calculated for those identified stars for which we have sufficient spectral type and apparent magnitude information. Distances were calculated using spectroscopic parallax, with an estimated uncertainty of $\Delta M_V = 1$. A comparison of these distances with those available from *Hipparcos* (see, e.g., Micela et al. 1997) gives reasonable agreement. Table 2 contains the stars for which both f_X/f_V and L_X could be determined.

4. NOTES ON INDIVIDUAL FIELDS

The results of our program of HRI observations are summarized in Table 3, which contains the positions of the detected HRI sources and other pertinent information. In addition, each field is discussed individually below.

1ES 0237−531.—The HRI observation was prompted by the presence of two possible optical counterparts in the ESS error circle (as discussed in SRSFSB), which are close enough to each other that they were both potential contributors to the ESS source. These two candidates are the binary system HD 16699 (F8 IV with a G or K companion) and the star SAO 232842, listed as K5 in the SAO catalog,

TABLE 2

LUMINOSITIES AND FLUX RATIOS

1ES Source	HD No.	Type	m_V	log (f_X/f_V)	Distance (pc)	log L_X[a]
0426−131.....	28497	B2 Vne	5.60	−5.32	500	30.6
0629+068.....	46122	G3 IV	7.6	−3.17[b]	95	30.4
0637−614.....	48189	G1.5 V	6.18	−3.08	21	29.8
0640+059.....	48393	G5 III	7.1	−4.73[b]	190	29.7
0717−572.....	57555	G0 IV/V	8.0	−2.56	74	30.6
1002−559.....	87525	K1/K2 III	8.0	−2.86	350	31.7
1339−688.....	119022	G2 IV/V	7.7	−2.84	59	30.3
1414−197[c].....	125048	A5 IV	6.9	−3.98	130	30.2
1456−400[d].....	132264	G8 IV	9.7	−3.07	200	30.4
1456−400[d].....	132349	F7/F8 V	10.1	−2.48	170	30.7

[a] Luminosity in ergs s^{-1}; values are lower limits.
[b] Averaged over two HRI observations.
[c] Another HRI source contributes; see § 4.
[d] Both stars contribute to ESS source; see § 4.

TABLE 3

POSITIONS OF HRI DETECTED SOURCES

Einstein IPC		*ROSAT* HRI			RASS		IDENTIFICATION	
1ES Name	Rate[a]	R.A.[b]	Decl.[b]	Rate	1RXS Name	Rate	Other Name	Type
0237−531.....	640 ± 240	2 38 45.22	−52 57 08.94	263 ± 8	J023845.4−525710	857 ± 80	SAO 232842	K5
							HD 16699	F8 IV/V
0426−131.....	120 ± 50	4 29 06.72	−13 02 53.41	6 ± 2	None[c,d]	<9	HD 28497[e]	B2 V
0437−046.....	500 ± 160	4 39 29.89	−4 35 56.97	134 ± 4	J043929.5−043605	212 ± 22	BF Eri[e]	Unknown
0524−711.....	120 ± 40	5 24 01.57	−71 09 32.65	56 ± 5	J052402.6−710956	328 ± 19	...	dM5e[e]
0629+068.....	160 ± 60	6 31 45.99	6 47 10.33	116 ± 9	J063145.8+064706	447 ± 32	HD 46122[e]	G3 IV
				132 ± 9				
0637−614.....	560 ± 150	6 38 00.16	−61 31 58.30	600 ± 17	J063800.7−613156	2325 ± 50	HD 48189[e]	G1.5 V
0640+059.....	100 ± 40	6 43 26.87	5 50 54.91	4 ± 1	None[c,d]	<11	HD 48393[e]	G5 III
				10 ± 2		<31		
0717−572.....	480 ± 160	7 18 27.44	−57 21 04.69	300 ± 14	J071827.7−572101	779 ± 34	HD 57555[e]	G0 IV/V
1002−559.....	430 ± 170	10 03 52.57	−56 11 19.73	186 ± 6	J100352.1−561134	586 ± 51	HD 87525[e]	K1/K2 III
1126−610.....	100 ± 40	No HRI sources[d]		<7; <4		None[e]		
1147−625.....	310 ± 80	No HRI sources[d]		<21		None[e]		
1212+078.....	250 ± 110	12 15 11.08	7 32 09.47	143 ± 7	J121510.9+073205	365 ± 32	...	BL Lac[e]
1339−688.....	800 ± 420	13 43 09.13	−69 07 32.92	255 ± 15	J134306.8−690754	844 ± 84	HD 119022[e]	G2 IV/V
1437−252.....	820 ± 440	No HRI sources[d]		<4		None[e]		
1414−197.....	260 ± 100	14 17 27.56	−19 57 46.06	39 ± 4	J141728.2−195751	180 ± 26	HD 125048	A5 IV
1456−400.....	750 ± 370	14 59 22.86	−40 13 12.51	64 ± 8	J145923.0−401319	187 ± 27	HD 132264	G8 IV
		14 59 52.66	−40 11 57.70	24 ± 5	J145951.7−401158	85 ± 19	HD 132349	F7/F8 V

NOTE.—Count rates in counts ks^{-1}. Units of right ascension are hours, minutes, and seconds, and units of declination are degrees, arcminutes, and arcseconds (J2000.0).
[a] Because of the Poisson distribution of counts, lower error estimates are actually somewhat smaller.
[b] Typical statistical position errors are $\leq 2''$, but the systematic uncertainty in absolute *ROSAT* HRI position can be as large as $10''$.
[c] See § 4 for notes on individual sources.
[d] Corresponding rate value represents the 3 σ upper limit.
[e] Confirms ESS identification.

but appearing to be of earlier spectral type ($\sim$G8) in the low-resolution spectra of SRSFSB. The optical spectra of both stars in the binary system show no visible signs of activity (i.e., chromospheric fill-in of lines), and HD 16699 was chosen as the "nominal" optical counterpart by SRSFSB on the basis of its proximity to the nominal position of the ESS X-ray source and of its higher $v \sin i$. However, as indicated by SRSFSB, the high-resolution spectrum of SAO 232842 shows the presence of measurable lithium, indicating a young age for a late-G star and making it a candidate counterpart.

We obtain a single detection for this ESS source, but neither the standard analysis nor the wavelet source detection algorithm is able to resolve the source. HD 16699 and SAO 232842 are positioned at 7″ and 13″, respectively, from the ESS source, defining an axis along which the HRI photon distribution is slightly elongated. Although the intrinsic resolution of the *ROSAT* HRI detector is capable of resolving objects this close together, uncertainties are introduced during the process of applying the *ROSAT* attitude solution to reconstruct the image. This typically results in a spatial resolving power no better than about 6″, or even more. Hence the ambiguity in the identification of this optical counterpart remains. Given the lesser resolution of the PSPC, the RASS BSC also detected a single counterpart for this ESS source.

1ES 0426−131.—In addition to the bright B2ne star HD 28497 identified by SRSFSB as the possible counterpart of this ESS source, three late-type stars ($V \sim 12$) present in the ESS error circle have optical low-resolution spectra with no signs of activity (one of these is significantly closer to the nominal ESS source position than HD 28497). On the basis of their f_X/f_V, however, they would be capable of producing at least part of the observed ESS flux. The HRI source 3″ from the listed position of HD 28497 (well within the HRI's position uncertainty of approximately 6″) is the only detected source within 2′ of the field center, thus confirming it unambiguously as the counterpart. The RASS exposure time estimated from the BSC (240 s), along with the HRI-PSPC count rate relation from Figure 1, predicts about five RASS counts for the source, below the detection threshold of 15 photons and consistent with the absence of a RASS counterpart.

1ES 0437−046.—The HRI position confirms the identification with BF Eri with a 15″ offset (SRSFSB). The source's optical spectrum (see Fig. 4 of SRSFSB), with its broad Balmer lines in emission, shows it to be a cataclysmic variable and, thus, not really a coronal source. This source is also present in the RASS BSC.

1ES 0524−711.—The SRSFSB identification with the dMe counterpart was rendered ambiguous by the presence in the ESS error circle of a relatively bright G star (incorrectly listed as B in the SIMBAD catalog). The HRI source position confirms the dMe star as the only X-ray source. The dMe star had already been identified as an X-ray source by Cowley et al. (1984). Using their value for the B magnitude of the star, as well as a $B-V$ index of $\simeq 1.5$ (reasonably constant for M dwarfs) and an approximate value for the bolometric corrections of ~ 1.7 (made rather uncertain by the lack of knowledge of an accurate spectral type for the source), we derive a f_X/f_{bol} ratio for this star of $\sim 10^{-2.6}$. This value is in the upper range of those observed for solar neighborhood dwarfs by Barbera et al. (1993), but it is not exceptional.

1ES 0629+068.—The HRI source position confirms the previous ESS identification with the G3 IV star HD 46122. The HRI source is $\sim 5''$ from the cataloged optical position of HD 46122 in the two observations, and a RASS X-ray source was also found.

1ES 0637−614.—The optical counterpart listed in SRSFSB (HD 48189, G1.5 V) is a close binary, with separation 0.″8 (ESA 1997) and $\Delta m = 2.3$ mag. In addition, a fainter ($V = 8.8$) late-type star lies in the ESS error circle, north of HD 48189. Neither of the two candidate counterparts shows signs of activity in low-resolution optical spectra. The HRI observation taken to resolve the ambiguity in optical identification confirms HD 48189 as the optical counterpart of the HRI source. An X-ray source is also present in the RASS BSC.

1ES 0640+059.—HRI positions $\sim 4''$ from the optical position confirm the ESS identification with the G5 III star HD 48393. No RASS X-ray source was detected, but from the exposure time of 364 s of this area in the RASS (W. Voges 1997, private communication), together with the estimated RASS count rate from the relation in Figure 1, we predict that the PSPC would have detected 4 and 11 counts in the two different HRI observations, i.e., below (perhaps marginally) the RASS BSC 15 count detection threshold photons; hence, the absence of detection is not surprising.

1ES 0717−572.—In addition to the optical counterpart listed in Table 1 of SRSFSB (HD 57555, G0 IV) a second slightly fainter, late-F star is present in the ESS error circle. Neither of the two candidate counterparts showed signs of activity in low-resolution optical spectra, making identification problematic. The HRI observation identifies HD 57555 as the true counterpart, and a RASS BSC counterpart is also present.

1ES 1002−559.—SRSFSB list the newly identified likely RS CVn-type system (SB2 system with K III primary, period unknown) HD 87525 as the prime candidate optical counterpart. However, the HRI observation was prompted by the presence of a late F star in the ESS error circle as a way to assess whether the F star is also an X-ray emitter. Finding the HRI source only 4″ from the position of HD 87525 rules out the F star as a contributor to the ESS source. This source is also present in the RASS BSC.

1ES 1126−610.—This source was noted in SRSFSB as a possible A-star X-ray emitter (HD 306536), but given that A stars are not normally seen as X-ray sources, an HRI observation was proposed to confirm the identification. Two separate HRI observations were made of this ESS source, for a total of 2 ks (898 + 1060 s), but there was no detection compatible with the ESS source position. Our 3 σ HRI upper limits for the A star are 6.0 and 4.7 counts for the two observations, respectively, a factor of about 50 below the values of 280^{+180}_{-148} and 331^{+212}_{-175} expected from the IPC-HRI rate relation given in Figure 2 and the ESS IPC count rates of 370^{+170}_{-140} counts ks^{-1}. There is also no RASS BSC detection in the vicinity. Given nondetections in both the HRI and PSPC, we conclude either that the ESS detected a transient source or, possibly, that the ESS detection (and therefore its proposed identification with the A star) may have been spurious.

1ES 1147−625.—This field was previously observed with the IPC and a source was detected, i.e., 2E 1147.6−6230 (*Einstein* 2E catalog, Harris et al. 1993). The 2E source has an IPC count rate of 67 ± 11 counts ks^{-1} and is located less than 30″ from the ESS source. It is in a region of diffuse

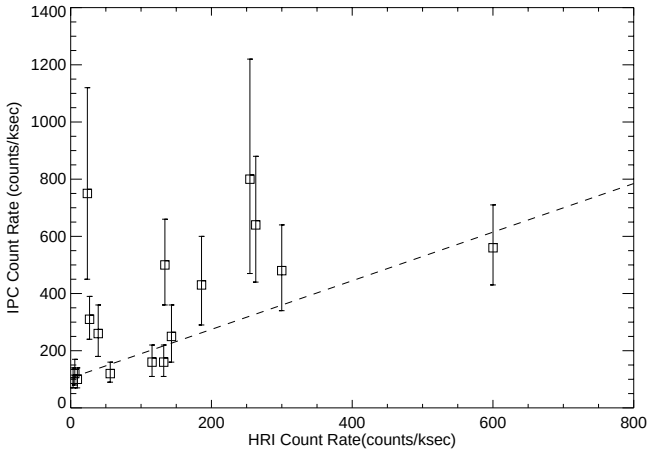

FIG. 2.—Observed IPC count rates from the ESS vs. *ROSAT* HRI count rates. The dashed line represents a weighted least χ^2 fit: IPC rate = 0.85(HRI rate) + 104, with both rates in counts ks^{-1}. Note that ESS rates were derived from IPC PI bins 1–15 and are therefore ~20% higher than those for the standard 0.2–4.0 keV interval (see col. [4] of Table 6 in Elvis et al. 1992).

X-ray emission near the supernova remnant (SNR) G296.1−0.5, which was also detected in the ESS as 1ES 1148−624 (SRSFSB). The ESS source 1ES 1147−625 was identified as the B9 V star HD 102867, which is optically positioned 1.'9 away from the ESS source.

Unfortunately, the HRI observed this field for only 235 s, shorter than requested. A low-confidence X-ray source is detected near the center, with an HRI count rate of 27 ± 11 counts ks^{-1}. Using the ESS count rate of 310^{+80}_{-70} counts ks^{-1}, we predict 57^{+22}_{-19} HRI photons. No RASS BSC source is present. From the 278 s RASS exposure time of this area (W. Voges 1997, private communication), we infer that the PSPC would have detected 24 ± 10 photons. Diffuse emission (likely due to the presence of the SNR) is also detected in the HRI field by both the standard and the wavelet analyses.

If we assume that the HRI point or diffuse detections represent the ESS counterpart, the HRI positions would be too far from that of HD 102867 to validate the ESS identification with the star. Given the low statistical significance of the ESS source and the position offset from the B9 V star, we conclude that 1ES 1147−625 was misidentified in the ESS and that the ESS detection represents either a transient source or a spurious point-source detection triggered by diffuse emission from G296.1−0.5. The 3 σ HRI upper limit derived for the optical position of HD 102867 is 21 counts ks^{-1}.

1ES 1212+078.—The ESS source was initially identified with the nearby K star SAO 119284. Radio emission was seen by Perlman et al. (1996), however, who identified it with a BL Lac object. There is an HRI detection 26″ from center, consistent with the position of the BL Lac object and with that of the corresponding RASS counterpart, which has a consistent PSPC count rate.

1ES 1339−688.—SRSFSB reported the presence of two G stars of comparable magnitude within the ESS error circle, as well as an early M star with weak Balmer emission. The proposed identification with HD 119022 rested on its being closer to the nominal ESS source position, although the dMe star was also considered a strong potential candidate counterpart. The HRI source is 6″ from the listed optical position of HD 119022, confirming the previous identification and ruling out the dMe star. A corresponding RASS BSC X-ray source was found.

1ES 1414−197.—Because Elvis et al. (1992) identified this source with the A5 IV star HD 125048, an HRI observation was conducted to confirm the possibility of unusual X-ray emission from this A-type star. The HRI observation confirms X-ray emission from a source located only 3″ from the listed optical position of HD 125048. There is also a RASS BSC counterpart. Since no information is currently available in the literature on the (possible) binary status of HD 125048, it is not possible to establish whether the X-ray emission emanates from the A star itself or from an unseen companion.

1ES 1437−252.—The original identification with the F0 V/F2 V star HD 129009 was made on the basis of positional coincidence (Elvis et al. 1992; SRSFSB). However, the implied f_X/f_V value was very high for a star of this spectral class, making the identification suspect. In a 1.28 ks HRI observation of this ESS field, there was no detection, nor was a RASS counterpart found. Given the lack of *ROSAT* detections and the low number of slew photons (only five), we suggest either that this ESS detection stemmed from a transient source or was a spurious detection. The 3 σ HRI upper limit for HD 129009 is 4.2 counts ks^{-1}.

1ES 1456−400.—The ESS gave the F7/F8 V star HD 132349 as the identification for this source. Both an HRI source and a RASS counterpart (with an HRI-consistent flux) were found, and a better position for the RASS source is therefore obtained from this observation. Identification with HD 132349 (offset by only 16″) is confirmed. (Note that a second detection in this field also revealed the G8 IV star HD 132264 as an X-ray source with a RASS counterpart, at about a third the intensity of the F-star system.)

5. DISCUSSION

5.1. *Spectral Characteristics of this Stellar Sample*

The slope of the PSPC versus HRI empirical relation (Fig. 1) encodes information about the intrinsic spectral properties of the observed stars, the intervening interstellar absorption (if any), and the relative instrumental responses of the *ROSAT* PSPC and HRI detectors. Since the calibrations of the two instruments are relatively well known, and since the assumption of negligible absorption is well justified for these relatively nearby objects, the observed

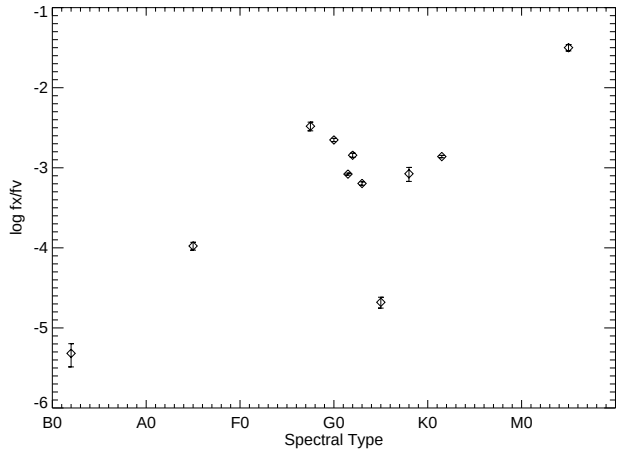

FIG. 3.—Plot of log (f_X/f_V) vs. spectral type for stars examined here

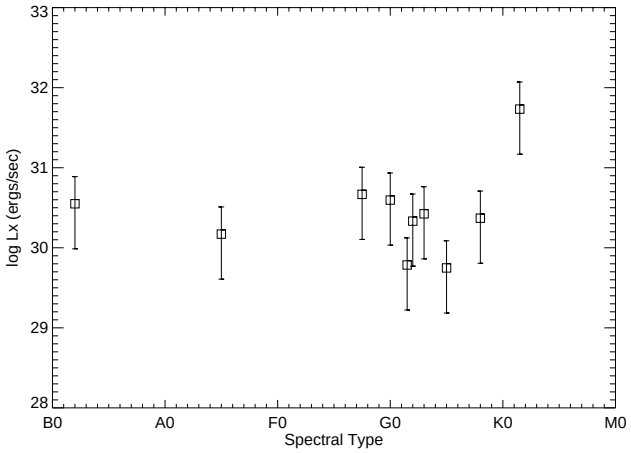

FIG. 4.—Plot of log L_X vs. spectral type for stars whose distance could be determined via spectroscopic parallax. Distance determination errors are indicated.

PSPC-to-HRI ratio permits us to infer a characteristic temperature of $kT \sim 0.8$ keV (for a single-temperature Raymond-Smith spectrum). This temperature is somewhat hotter than that of typical coronal sources, as expected for the sources selected in this work. Because of the relative insensitivity of the ESS, only the more active (or flaring) stars, with their higher temperatures, could be detected.

5.2. *X-Ray and Optical Fluxes*

We have computed ratios of X-ray to optical flux, f_X/f_V, for each of our detected sources and display the results in Figure 3. The observed behavior is typical of the stellar components of both the ESS (SRSFSB) and the *Einstein* Extended Medium-Sensitivity Survey (EMSS; Fleming, Gioia, & Maccacaro 1989). For instance, the f_X/f_V distribution of Figure 3 is precisely what the EMSS shows for stars of relatively bright magnitude (cf. Figs. 1 and 2 in Micela et al. 1997). Individual X-ray luminosities are shown in Figure 4, where the values of L_X are uncertain by about a factor of 2, because of uncertainties in the spectroscopic parallax distances and the count rate–to–flux conversion factor. Here as well, the values are at the high end of normal coronal sources, a result of the selection effects of the Slew Survey.

5.3. *X-Ray Emission from A-Type Stars*

Two ESS sources had been identified with A-type counterparts. Although one (1ES 1126−610; see above) may represent a spurious X-ray detection, the other persists under the scrutiny of the HRI. Identified with HD 125048, 1ES 1414−197 has a rather high X-ray luminosity of $L_X \sim 10^{30}$ ergs s^{-1}, making this a puzzling source indeed. Although nothing is presently known in the literature about this A star, emission from an unseen companion is an obvious possibility.

6. CONCLUSIONS

The goal of this program of HRI observations was to determine unique optical counterparts for several ESS X-ray detections that SRSFSB found to be ambiguous because of their large error circles. In all of the cases, however, a "most plausible" counterpart had been identified by SRSFSB, based on criteria of positional coincidence, the presence of optical spectra activity indicators, and the X-ray emission level for the spectral class.

The results of the program confirm the soundness of the approach taken by SRSFSB: for the 16 ESS sources studied here, in 10 cases the previous identifications have been confirmed, while in two other cases both candidate optical counterparts identified have been shown to be X-ray sources (1ES 1414−197, 1ES 1456−400). In one more case (1ES 0237−151) the two optical candidates are so close together that even the HRI is unable to resolve the ambiguity, although the distribution of HRI photons suggests both as possible contributors. Finally, in the three remaining cases, the ESS detections have been deemed transient or spurious, with two cases yielding no HRI detection (1ES 1126−610, 1ES 1437−252) and one case showing diffuse X-ray emission (from a known SNR) that may have been spuriously interpreted in the ESS as a point source (1ES 1147−625). Thus, in the large majority of cases the identification made by SRSFSB proved correct. The question of X-ray emission from A-type stars such as HD 125048 (1ES 1414−197) remains to be addressed, hopefully, by upcoming X-ray observatories such as the *Chandra X-Ray Observatory* (formerly *AXAF*) and the *XMM*.

This work was supported in part under NSF grant AST 93-21943 and NASA grants NAG 5-2644 and NAG 5-4967. G. M. and S. S. acknowledge partial support from the Italian Space Agency and the Ministero dell'Università e della Ricerca Scientifica e Tecnologica. We would like to thank W. Voges for the RASS exposure times, Jonathan McDowell for his assistance with LaTeX and IRAF, and R. Hank Donnelly for his invaluable help with IRAF and for proofreading early versions of the manuscript.

The Digitized Sky Surveys and Hubble Guide Star Catalog were produced at the Space Telescope Science Institute under US government grant NAG W-2166. The images of these surveys are based on photographic data obtained using the Oschin Schmidt Telescope on Mount Palomar and the Schmidt Telescope in the UK. The plates were processed into the present compressed digital form with the permission of these institutions. This research has made use of the SIMBAD database, operated at CDS, Strasbourg, France, and also the High Energy Astrophysics Science Archive Research Center Online Service (HEASARC), provided by the NASA Goddard Space Flight Center.

REFERENCES

Barbera, M., Micela, S., Sciortino, S., Harnden, F. R., Jr., & Rosner, R. 1993, ApJ, 414, 846
Berghöfer, T. W., Schmitt, J. H. M. M., & Cassinelli, J. P. 1996, A&AS, 118, 481
Cowley, A. P., Crampton, D., Hutchings, J. B., Helfand, D. J., Hamilton, T. T., Thorstensen, J. R., & Charles, P. A. 1984, ApJ, 286, 196
Damiani, F., Maggio, A., Micela, G., & Sciortino, S. 1997, ApJ, 483, 350
David, L. P., Harnden, F. R., Jr., Kearns, K. E., & Zombeck, M. V. 1997, The ROSAT High Resolution Imager (HRI) Calibration Report (Cambridge: US *ROSAT* Sci. Data Cent.)
Downes, R., White, R., Reichert, G., Dennerl, K., Englhauser, J., Rosso, C., & Voges, W. 1994, The *ROSAT* Data Products Guide (version 7.0; Garching: MPI extraterr. Phys)
Elvis, M., Plummer, D., Schachter, J., & Fabbiano, G. 1992, ApJS, 80, 257
ESA. 1997, The Hipparcos and Tycho Catalogues (ESA SP-1200) (Noordwijk: ESA)
Favata, F., Barbera, M., Micela, G., & Sciortino, S. 1995, A&A, 295, 147
Flaccomio, E., et al. 1999, in preparation
Fleming, T., Gioia, I., & Maccacaro, T. 1989, AJ, 98, 692
Giacconi, R., et al. 1979, ApJ, 230, 540

Gorenstein, P., Harnden, F. R., Jr., & Fabricant, D. G. 1981, IEEE Trans. Nucl. Sci., 28, 869
Harnden, F. R., Jr., Fabricant, D. G., Harris, D. E., & Schwarz, J. 1984, Scientific Specification of the Data Analysis System for the *Einstein Observatory* (*HEAO*-2) Imaging Proportional Counter (Cambridge: Smithsonian Astrophys. Obs.)
Harris, D. E., et al. 1993, The *Einstein Observatory* Catalog of IPC X-Ray Sources (NASA Tech. Mem. 108401, 7 vols. (Cambridge: Smithsonian Astrophys. Obs.)
Lasker, B. M., et al. 1988, ApJS, 68, 1
Micela, G., Favata, F., & Sciortino, S. 1997, A&AS, 326, 221
Perlman, E. S., et al. 1996, ApJS, 104, 251
Pfeffermann, E., & Briel, U. G. 1986, Proc. SPIE, 597, 208
Plummer, D., Schachter, J., Garcia, M., Elvis, M., & McDowell, J., eds., 1992, The *Einstein Observatory* Database of HRI Images in Event List Format (FITS binary table CD-ROM; Cambridge: Smithsonian Astrophys. Obs.)
Schachter, J. F., Remillard, R., Saar, S. H., Favata, F., Sciortino, S., & Barbera, M. 1996, ApJ, 463, 747 (SRSFSB)
Voges, W., et al. 1996, IAU Circ. 6420
Zombeck, M. V., Conroy, M., Harnden, F. R., Jr., Roy, A., Braeuninger, H., Burkert, W., Hasinger, G., & Predehl, P. 1990, Proc. SPIE, 1344, 267